Bol. Soc. Paran. Mat.
©SPM – E-ISSN-2175-1188
SPM: www.spm.uem.br/bspm

(3s.) **v. 2026 (44)** : 1–18.
ISSN-0037-8712
doi:10.5269/bspm.77860

Investigation of Reverse Degree Based Polynomials & Structural Descriptors of Silicate Chain, Network and Silicate Triangle Fractal Network

Gayathiri Vasudevan, Manimaran Angamuthu*, Abdul Rauf Khan, Farhan Qadir

ABSTRACT: Chemical graph theory is experiencing a surge in the numerical encoding of chemical structures using topological indices. These topological indices have a crucial component that has to do with predicting the feature provided by the molecule's chemical structure. The topological indices of silicate networks, silicate chains and silicate triangle fractal network are computed in this research using a specially devised approach called reverse degree-based topological indices. Also, the calculated reverse degree-based topological indices will be compared with the number of silicate structure copies in each iteration involving silicon within the silicate triangle fractal network graph sequence.

Keywords: Silicate, chain, network, silicate triangle fractal network, reverse degree, molecular structural descriptors, polynomials, computation.

Contents

1. Introduction

Graph theory was first studied in 1735 when it was used for the Koinsberg bridge problem. Currently, graph theory finds use in various domains, including biology, chemistry, computer science, and engineering. Graph theory is an effective tool for modeling chemical structures, creating intricate networks, and resolving everyday issues. Balaban [1], Graovac [2], Gutman [3], Hosoya, Randic [4], and Trinajstic [5,6,7] are credited with inventing chemical graph theory, which has grown to be a significant section of mathematical chemistry. A useful technique for creating new molecular structures and molecular modeling is chemical graph theory, which transforms molecular information into mathematical equations and numbers [8]. A basic graph, devoid of loops or numerous edges, is used in chemical graph theory to depict the structure of molecules [9,10]. The edges of the graphical structure in a chemical compound indicate the chemical bonds that hold the atoms in the molecule together, while the vertices of the graphical structure express the atom. If there is a contact between each pair of vertices in graph G, where a set of edges is represented by $E(G)$ and a set of vertices is represented by $V(G)$, then the graph $G(V, E)$ is said to be connected. Once chemical information of a chemical structure is converted into an important number, a logical and mathematical process yields the topological index for the chemical graph [11]. These topological indices are widely used in QSAR and QSPR investigations. QSAR & QSPR applied

* Corresponding author.
2020 *Mathematics Subject Classification:* 05C92, 92E10, 28A80.
Submitted July 15, 2025. Published March 19, 2026

to Biological activity and Physical, chemical, or material properties of molecules. QSAR is focused on predicting absorption, Distribution, Metabolism, Excretion, and Toxicity properties. It estimates models' surface energy, particle size effects, and catalytic properties. Moreover, predict conductivity, ion transport efficiency, and stability. QSPR predicts measurable properties (physical/chemical). It estimates the harmful effects of chemicals on aquatic and terrestrial organisms.

An index that is determined by utilizing the degrees of vertices in the graphical structure of a chemical compound is known as a degree-dependent topological index [12]. To predict the topological features of chemical graphs and networks and to comprehend structural activity relations, computer-aided design, and medication creation, degree-dependent topological indices are typically utilized [13]. The inherent chemical and physical properties of the relevant chemical compounds and nanostructures can be predicted with the help of topological descriptors, sometimes referred to as topological indices, which are frequently employed mathematical tools in contemporary literature. It is discovered that several characteristics correlate with these indices, including stiffness, fracture toughness, boiling point, and strain energy [14,15]. The degree of vertices and edges, as well as distance, are some of the invariants that form the basis of these indexes. Some well-known topological indices in literature are Wiener indices, Randic indices, Hosoya indices, and Zagreb indices. $\beta(V, D)$ represents the molecular graph, where $V(\beta)$,$D(\beta)$ indicate the vertex and edge set, and $V(\beta)$,$D(\beta)$ indicate the order and size of β. Let Φ_v be the degree of the vertex v and $\Delta(\beta)$ be the graph's maximum degree. The formula for a vertex v reverse degree is [26]

$$R_v = \Delta(\beta) - \Phi_v + 1$$

Zhao et al in [16]. The reverse 1st and 2nd Zagreb index [17], the reverse 1^{st} and 2^{nd} hyper Zagreb index, the reverse 1^{st}, 2^{nd}, and 3^{rd} redefined Zagreb index, the reverse atom bond connectivity index, and the reverse Zagreb type indices were computed. These were among the reverse degree-based topological indices (RDBTs) that were determined.

2. Material and Methodology

In this section, we describe the material and methodology.

2.1. Silicate Network, Silicate Chain and Silicate triangle fractal network

Rock-forming minerals made up of silicate groups are called silicate minerals. They belong to the most significant and prevalent class of minerals [18]. A total of 78 mineral classes exist. Of them, 27 are silicates, which make up almost two-thirds of the crust of the earth. Sand is combined with metal carbonates or oxides to create silicates. SiO_4,which has a tetrahedron structure, is the basic chemical unit of silicates [19]. While oxygen ions occupy the tetrahedron's end vertices, silicon ions occupy the central vertex of the SiO_4 tetrahedron. The building blocks of a silicate sheet are rings of tetrahedrons connected in a two-dimensional plane by oxygen ions, which combine to produce a structure resembling a sheet [27]. Assumed to be a distinct network of parallel construction, the silicate sheet is also referred to as a silicate network [20]. The symbol for the silicate network SL_n, where n is the number of hexagons that are present between the network's center and boundary. The two-dimensional silicate network is shown in Figure 1. In Figure 1, the vertices of degrees three and six are indicated by green and pink dots, respectively, and the edges with degrees of end vertices (3, 3), (3, 6) and (6, 6) are indicated by black lines.

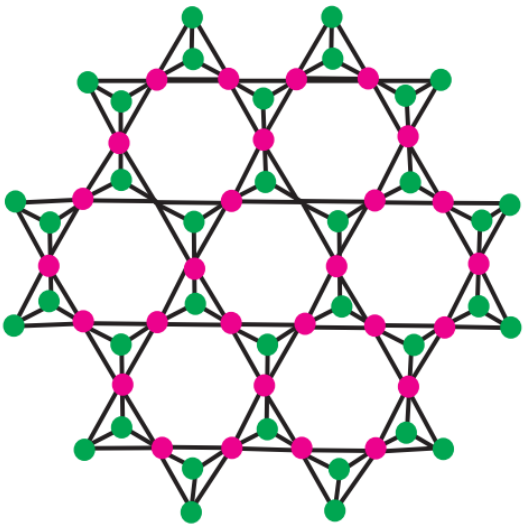

Figure 1: Silicate Network SL_n for $n = 2$

The chain of silicates (SLC) that results are now SC_s^r, where s and r represent the number of silicate chains formed of the total number of SiO_4 in a single silicate chain and sr number of tetrahedron SiO_4 is used in the chain of silicates SC_s^r as illustrated in Figure 2. Based on the valency of each atom in the chain of silicates SC_s^r, we have noticed that there exist three different types of atom bonds. The valency of atoms ui, uj to SC_s^r is represented by d_ui and d_uj, meaning that there exist two types of atoms, ui and uj, such that $d_ui = 3$ and $d_uj = 6$. In SC_s^r, there are three sorts of atom bonds: (3, 3), (3, 6) and (6, 6) based on the valencies (3, 6) of the atoms. On the base of valency, Table 2 provides the partition.

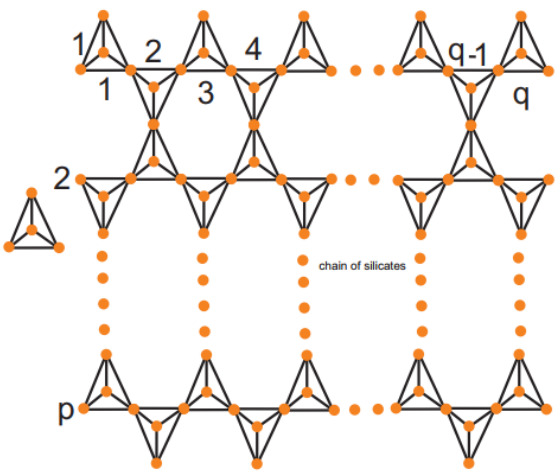

Figure 2: Chain of Silicate Network

The silicate sheet converts as a fractal network, it resembles the Sierpiński triangle [21]. The silicate triangle fractal network, denoted as Si_n is constructed through iterative fractal graph formation, where $n = s$ represents the number of fractal iterations. The initial structure, Si_0 starts as an equilateral triangle with lines connecting the vertices to its center, resembling a Sierpiński triangle [22]. At each iteration, the corner oxygen atoms of each side produce three new silicates. so that Si_1 contains three silicates added to the original structure.

This iterative process continues, with each corner oxygen atom generating 3^n new silicates at the n^{th} level forming a progressively complex n-level silicate triangle fractal network, Si_n (as depicted in Figure 3). The Si_n contains $3(\frac{3^{n+1}-1}{2})+1$ vertices and $3(3^{n+1})-3$ edges. Thus, the fractal structure grows inclusively as $Si_0 \subseteq Si_1 \subseteq Si_2 \ldots$, with each iteration building upon the previous. This construction process theoretically continues indefinitely, producing an infinitely complex fractal network.

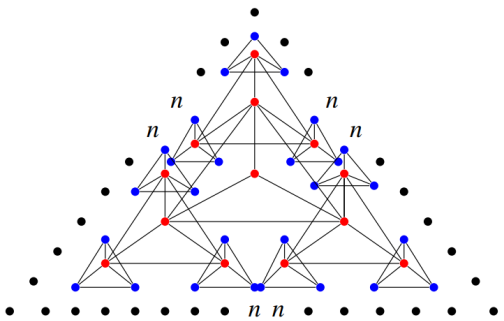

Figure 3: n^{th} iteration of Silicate triangle fractal network Si_n

2.2. Reverse Degree Based Polynomials & Descriptors

The following are the reverse degree-based indices which we have utilized in our study. Reverse degree–based indices can capture the complexity of fractal networks and correlate with Physical properties, Chemical properties and Biological activities.

RM_1 index is applied to graphene sheets, dendrimers, and carbon nanotubes. It is useful in analyzing hierarchical structures such as fractal networks. The Reverse 1^{st} Zagreb polynomial and index is expressed as [23].

$$RM_1(G,p) = \sum_{\alpha\gamma \in E(G)} p^{i\alpha+i\gamma} \quad \& \quad RM_1(G) = \sum_{\alpha\gamma \in E(G)} (i\alpha + i\gamma) \tag{2.1}$$

In communication or biological networks, RM_2 index helps identify weak link patterns. It supports extremal graph results on bounds and inequalities. The Reverse 2^{nd} Zagreb polynomial and index is defined as [23]

$$RM_2(G,p) = \sum_{\alpha\gamma \in E(G)} p^{i\alpha \cdot i\gamma} \quad \& \quad RM_2(G) = \sum_{\alpha\gamma \in E(G)} (i\alpha \cdot i\gamma) \tag{2.2}$$

RHM_1 index is used as an additional topological descriptor in multi-descriptor QSAR models to improve predictive accuracy. The Reverse 1^{st} hyper Zagreb polynomial and index is expressed as [23]

$$RHM_1(G,p) = \sum_{\alpha\gamma \in E(G)} p^{(i\alpha+i\gamma)^2} \quad \& \quad RHM_1(G) = \sum_{\alpha\gamma \in E(G)} (i\alpha + i\gamma)^2 \tag{2.3}$$

RHM_2 index predicts heat transfer, electrical conductivity and uses of Nanostructure optimization, extremal graph studies. The Reverse 2^{nd} hyper Zagreb polynomial and index is expressed as [23]

$$RHM_2(G,p) = \sum_{\alpha\gamma \in E(G)} p^{(i\alpha \cdot i\gamma)^2} \quad \& \quad RHM_2(G) = \sum_{\alpha\gamma \in E(G)} (i\alpha \cdot i\gamma)^2 \tag{2.4}$$

Redefined Zagreb indices are evaluated for bioactivity modeling for antimicrobial, anticancer, and antiviral compounds. The Reverse 1^{st}, 2^{nd}, 3^{rd} Redefined Zagreb polynomial and index is expressed as [24]

$$RReZG_1(G,p) = \sum_{\alpha\gamma \in E(G)} p^{\frac{(i\alpha+i\gamma)}{(i\alpha \cdot i\gamma)}} \quad \& \quad RReZG_1(G) = \sum_{\alpha\gamma \in E(G)} \frac{(i\alpha + i\gamma)}{(i\alpha \cdot i\gamma)} \tag{2.5}$$

$$RReZG_2(G,p) = \sum_{\alpha\gamma\in E(G)} p^{\frac{(i\alpha\cdot i\gamma)}{(i\alpha+i\gamma)}} \quad \& \quad RReZG_2(G) = \sum_{\alpha\gamma\in E(G)} \frac{(i\alpha\cdot i\gamma)}{(i\alpha+i\gamma)} \tag{2.6}$$

$$RReZG_3(G,p) = \sum_{\alpha\gamma\in E(G)} p^{(i\alpha\cdot i\gamma)(i\alpha+i\gamma)} \quad \& \quad RReZG_3(G) = \sum_{\alpha\gamma\in E(G)} (i\alpha\cdot i\gamma)(i\alpha+i\gamma) \tag{2.7}$$

Leveraging the $RABC$ index enables the prediction of characteristics influenced by the peripheral structure, such as solubility and surface reactivity. The Reverse Atom bond connectivity polynomial and index are expressed [25].

$$RABC(G,p) = \sum_{\alpha\gamma\in E(G)} p^{\sqrt{\frac{(i\alpha+i\gamma-2)}{(i\alpha\cdot i\gamma)}}} \quad \& \quad RABC(G) = \sum_{\alpha\gamma\in E(G)} \sqrt{\frac{(i\alpha+i\gamma-2)}{(i\alpha\cdot i\gamma)}} \tag{2.8}$$

Table 1: Reverse degree based edge partition of silicate network (SL_n)

Types of Atom Bonds	Cardinality
E(4,4)	6s
E(4,1)	6s(3s+1)
E(1,1)	6s(3s-2)

3. Reverse Degree Based TD's for Silicate Network

The Reverse 1^{st} Zagreb Polynomial and Index

Using Table 1 along with Equation (2.1), we get:

$$RM_1SL_n(P) = p^{(4+4)}(6s) + p^{(4+1)}6s(3s+1) + p^{(1+1)}6s(3s-2)$$

$$RM_1SL_n(P) = p^{(8)}(6s) + p^{(5)}6s(3s+1) + p^{(2)}6s(3s-2) \tag{3.1}$$

After simplification Equation (3.1), we get

$$\begin{aligned} RM_1SL_n(P) &= (8)(6s) + (5)6s(3s+1) + (2)6s(3s-2) \\ RM_1SL_n(P) &= 48s + 90s^2 + 30s + 36s^2 - 24s \\ RM_1SL_n(P) &= 126s^2 + 54s \end{aligned}$$

The Reverse 2^{nd} Zagreb Polynomial and Index

Using Table 1 along with Equation (2.2), we get:

$$RM_2SL_n(P) = p^{(4\cdot4)}(6s) + p^{(4\cdot1)}6s(3s+1) + p^{(1\cdot1)}6s(3s-2)$$

$$RM_2SL_n(P) = p^{(16)}(6s) + p^{(4)}6s(3s+1) + p^{(1)}6s(3s-2) \tag{3.2}$$

After simplification Equation (3.2), we get

$$\begin{aligned} RM_2SL_n(P) &= (16)(6s) + (4)6s(3s+1) + (1)6s(3s-2) \\ RM_2SL_n(P) &= 96s + 72s^2 + 24s + 18s^2 - 12s \\ RM_2SL_n(P) &= 90s^2 + 108s \end{aligned}$$

The Reverse 1^{st} hyper Zagreb Polynomial and Index

Using Table 1 alongwith Equation (2.3), we get Using Table 1 along with Equation (3), we get:

$$RHM_1SL_n(P) = p^{(4+4)^2}(6s) + p^{(4+1)^2}6s(3s+1) + p^{(1+1)^2}6s(3s-2)$$

$$RHM_1SL_n(P) = p^{(64)}(6s) + p^{(25)}6s(3s+1) + p^{(4)}6s(3s-2) \tag{3.3}$$

After simplification Equation (3.3), we get

$$\begin{aligned} RHM_1SL_n(P) &= (64)(6s) + (25)6s(3s+1) + (4)6s(3s-2) \\ RHM_1SL_n(P) &= 384s + 450s^2 + 150s + 72s^2 - 48s \\ RHM_1SL_n(P) &= 522s^2 + 486s \end{aligned}$$

The Reverse 2^{nd} hyper Zagreb Polynomial and Index

Using Table 1 along with Equation (2.4), we get

$$RHM_2SL_n(P) = p^{(4\cdot4)^2}(6s) + p^{(4\cdot1)^2}6s(3s+1) + p^{(1\cdot1)^2}6s(3s-2)$$

$$RHM_2SL_n(P) = p^{(256)}(6s) + p^{(16)}6s(3s+1) + p^{(1)}6s(3s-2) \tag{3.4}$$

After simplification Equation (3.4), we get

$$\begin{aligned} RHM_2SL_n(P) &= (256)(6s) + (16)6s(3s+1) + (1)6s(3s-2) \\ RHM_2SL_n(P) &= 1536s + 288s^2 + 96s + 18s^2 - 12s \\ RHM_2SL_n(P) &= 306s^2 + 1620s \end{aligned}$$

The Reverse 1^{st} redefined Zagreb Polynomial and Index

Using Table 1 along with Equation (2.5), we get

$$RReZG_1SL_n(P) = p^{\frac{(4+4)}{(4\cdot4)}}(6s) + p^{\frac{(4+1)}{(4\cdot1)}}6s(3s+1) + p^{(1+1)}(1\cdot1)6s(3s-2)$$

$$RReZG_1SL_n(P) = p^{\frac{(8)}{(16)}}(6s) + p^{\frac{(5)}{(4)}}6s(3s+1) + p^{\frac{(2)}{(1)}}6s(3s-2) \tag{3.5}$$

After simplification Equation (3.5), we get

$$\begin{aligned} RReZG_1SL_n(P) &= \frac{8}{16}(6s) + \frac{5}{4}6s(3s+1) + \frac{2}{1}16s(3s-2) \\ RReZG_1SL_n(P) &= 3s + \frac{90}{4}s^2 + \frac{30}{4}s + \frac{36}{1}s^2 - \frac{24}{1}s \\ RREZG_1SL_n(P) &= \frac{117}{2}s^2 - \frac{27}{2}s \end{aligned}$$

The Reverse 2^{nd} redefined reverse Zagreb Polynomial and Index

Using Table 1 along with Equation (2.6), we get

$$RReZG_2SL_n(P) = p^{\frac{(4\cdot4)}{(4+4)}}(6s) + p^{\frac{(4\cdot1)}{(4+1)}}6s(3s+1) + p^{\frac{(1\cdot1)}{(1+1)}}6s(3s-2)$$

$$RReZG_2SL_n(P) = p^{\frac{(16)}{(8)}}(6s) + p^{\frac{(4)}{(5)}}6s(3s+1) + p^{\frac{(1)}{(2)}}6s(3s-2) \tag{3.6}$$

After simplification Equation (3.6), we get

$$RReZG_2SL_n(P) = \frac{16}{8}(6s) + \frac{4}{5}6s(3s+1) + \frac{1}{2}6s(3s-2)$$
$$RReZG_2SL_n(P) = 12s + \frac{72}{5}s^2 + \frac{24}{5}s + \frac{18}{2}s^2 - \frac{12}{2}s$$
$$RReZG_2SL_n(P) = \frac{117}{5}s^2 + \frac{54}{5}s$$

The Reverse 3^{nd} redefined Zagreb Polynomial and Index
Using Table 1 along with Equation (2.7), we get

$$RReZG_3SL_n(P) = p^{(4\cdot4)}(4+4)6s + p^{(4\cdot1)}(4+1)6s(3s+1) + p^{(1\cdot1)}(1+1)6s(3s-2)$$

$$RReZG_3SL_n(P) = p^{(16)(8)}6s + p^{(4)(5)}6s(3s+1) + p^{(1)(2)}6s(3s-2) \tag{3.7}$$

After simplification equation (3.7), we get

$$RReZG_3SL_n(P) = (16)(8)6s + (4)(5)6s(3s+1) + (1)(2)6s(3s-2)$$
$$RReZG_3SL_n(P) = 768s + 360s^2 + 120s + 36s^2 - 24s$$
$$RReZG_3SL_n(P) = 396s^2 + 864s$$

The Reverse Atom bond connectivity polynomial and index
Using Table 1 along with Equation (2.8), we get:

$$RABCSL_n(P) = p^{\sqrt{\frac{(4+4-2)}{(4\cdot4)}}}(6s) + p^{\sqrt{\frac{(4+1-2)}{(4\cdot1)}}}6s(3s+1) + p^{\sqrt{\frac{(1+1-2)}{(1\cdot1)}}}6s(3s-2)$$

$$RABCSL_n(P) = p^{\sqrt{\frac{6}{16}}}(6s) + p^{\sqrt{\frac{3}{4}}}6s(3s+1) + p^{\sqrt{\frac{0}{1}}}6s(3s-2) \tag{3.8}$$

After simplification of Equation (3.8), we get:

$$RABCSL_n(P) = \sqrt{\frac{3}{8}}(6s) + \sqrt{\frac{3}{4}}6s(3s+1)$$

4. Reverse Degree Based TD's of Silicate Chain

Table 2: Reverse degree based edge partition of silicate chain (SC_s^r)

Types of Atom Bonds	Cardinality
E(4,4)	3s+2
E(4,1)	3(sr+r)-4
E(1,1)	3(sr-2r)+2

The Reverse 1^{st}-Zagreb polynomial and index
Using Table 2 along with Equation (2.1), we get:

$$RM_1SC_r^s(P) = p^{(4+4)}(3s+2) + p^{(4+1)}(3(sr+r)-4) + p^{(1+1)}(3(sr-2r)+2)$$

$$RM_1SC_r^s(P) = p^8(3s+2) + p^5(3(sr+r)-4) + p^2(3(sr-2r)+2) \tag{4.1}$$

After simplification of Equation (4.1), we get:

$$RM_1SC_r^s(P) = (8)(3s+2) + (5)(3(sr+r)-4) + (2)(3(sr-2r)+2)$$
$$RM_1SC_r^s(P) = 24s + 16 + 15sr + 15r - 20 + 6sr - 12r + 4$$
$$RM_1SC_r^s(P) = 24s + 21sr + 3r$$

The Reverse 2^{nd}-Zagreb polynomial and index

Using Table 2 along with Equation (2.2), we get:

$$RM_2SC_r^s(P) = p^{(4\cdot4)}(3s+2) + p^{(4\cdot1)}(3(sr+r)-4) + p^{(1\cdot1)}(3(sr-2r)+2)$$

$$RM_2SC_r^s(P) = p^{16}(3s+2) + p^{4}(3(sr+r)-4) + p^{1}(3(sr-2r)+2) \tag{4.2}$$

After simplification of Equation (4.2), we get:

$$RM_2SC_r^s(P) = (16)(3s+2) + (4)(3(sr+r)-4) + (1)(3(sr-2r)+2)$$
$$RM_2SC_r^s(P) = 48s + 32 + 12sr + 12r - 16 + 3sr - 6r + 2$$
$$RM_2SC_r^s(P) = 48s + 15sr + 6r + 18$$

The Reverse 1^{st}- hyper Zagreb polynomial and index

Using Table 2 along with Equation (2.3), we get:

$$RHM_1SC_r^s(P) = p^{(4+4)^2}(3s+2) + p^{(4+1)^2}(3(sr+r)-4) + p^{(1+1)^2}(3(sr-2r)+2)$$

$$RHM_1SC_r^s(P) = p^{(8)^2}(3s+2) + p^{(5)^2}(3(sr+r)-4) + p^{(2)^2}(3(sr-2r)+2) \tag{4.3}$$

After simplification of Equation (4.3), we get:

$$RHM_1SC_r^s(P) = (64)(3s+2) + (25)(3(sr+r)-4) + (4)(3(sr-2r)+2)$$
$$RHM_1SC_r^s(P) = 192s + 128 + 75sr + 75r - 100 + 12sr - 24r + 8$$
$$RHM_1SC_r^s(P) = 192s + 87sr + 51r + 36$$

The Reverse 2^{nd}- hyper Zagreb polynomial and index

Using Table 2 along with Equation (2.4), we get:

$$RHM_2SC_s^r(P) = p^{(4\cdot4)^2}(3s+2) + p^{(4\cdot1)^2}(3(sr+r)-4) + p^{(1\cdot1)^2}(3(sr-2r)+2)$$

$$RHM_2SC_s^r(P) = p^{256}(3s+2) + p^{16}(3(sr+r)-4) + p^{1}(3(sr-2r)+2) \tag{4.4}$$

After simplification of Equation (4.4), we get:

$$RHM_2SC_s^r(P) = 256(3s+2) + 16(3(sr+r)-4) + 1(3(sr-2r)+2)$$
$$RHM_2SC_s^r(P) = 768s + 512 + 48sr + 48r - 64 + 3sr - 6r + 2$$
$$RHM_2SC_s^r(P) = 768s + 51sr + 42r + 450$$

The Reverse 1^{st} redefined Zagreb Polynomial and Index

Using Table 2 along with Equation (2.5), we get:

$$RReZG_1SC_s^r(P) = \sum_{(4,4)\in(G)} p^{\frac{(c_4+c_4)}{(c_4\cdot c_4)}} + \sum_{(4,1)\in(G)} p^{\frac{(c_4+c_1)}{(c_4\cdot c_1)}} + \sum_{(1,1)\in(G)} p^{\frac{(c_1+c_1)}{(c_1\cdot c_1)}}$$
$$RReZG_1SC_s^r(P) = p^{\frac{(4+4)}{(4\cdot4)}}(3s+2) + p^{\frac{(4+1)}{(4\cdot1)}}(3(sr+r)-4) + p^{\frac{(1+1)}{(1\cdot1)}}(3(sr-2r)+2)$$
$$RReZG_1SC_s^r(P) = p^{\frac{8}{16}}(3s+2) + p^{\frac{5}{4}}(3(sr+r)-4) + p^{\frac{(2)}{1}}(3(sr-2r)+2) \tag{4.5}$$

After simplification of Equation (4.5), we get:

$$RReZG_1SC_s^r(P) = \frac{8}{16}(3s+2) + \frac{5}{4}(3(sr+r)-4) + \frac{2}{1}(3(sr-2r)+2)$$
$$RReZG_1SC_s^r(P) = \frac{24s}{16} + 1 + \frac{15sr}{4} + \frac{15r}{4} - 5 + 6sr - 12r + 4$$
$$RReZG_1SC_s^r(P) = \frac{24s}{16} + \frac{39sr}{4} - \frac{33r}{4}$$

The Reverse 2^{nd} redefined Zagreb Polynomial and Index

Using Table 2 along with Equation (2.6), we get:

$$RReZG_2SC_s^r(P) = \sum_{(4,4)\in(G)} p^{\frac{(c_4\cdot c_4)}{(c_4+c_4)}} + \sum_{(4,1)\in(G)} p^{\frac{(c_4\cdot c_1)}{(c_4+c_1)}} + \sum_{(1,1)\in(G)} p^{\frac{(c_1\cdot c_1)}{(c_1+c_1)}}$$
$$RReZG_2SC_s^r(P) = p^{\frac{(4\cdot 4)}{(4+4)}}(3s+2) + p^{\frac{(4\cdot 1)}{(4+1)}}(3(sr+r)-4) + p^{\frac{(1\cdot 1)}{(1+1)}}(3(sr-2r)+2)$$
$$RReZG_2SC_s^r(P) = p^{\frac{16}{(8)}}(3s+2) + p^{\frac{4}{(5)}}(3(sr+r)-4) + p^{\frac{1}{(2)}}(3(sr-2r)+2) \quad (4.6)$$

After simplification of Equation 4.6 we get:

$$RReZG_2SC_s^r(P) = \frac{16}{8}(3s+2) + \frac{4}{5}(3(sr+r)-4) + \frac{1}{2}(3(sr-2r)+2)$$
$$RReZG_2SC_s^r(P) = 6s + 4 + \frac{12sr}{5} + \frac{12r}{5} - \frac{16}{5} + \frac{3sr}{2} - \frac{6r}{2} + 1$$
$$RReZG_2SC_s^r(P) = 6s + \frac{39sr}{10} - \frac{3r}{5} + \frac{9}{5}$$

The Reverse 3^{nd} redefined Zagreb Polynomial and Index

Using Table 2 along with Equation (2.7), we get:

$$RReZG_3SC_s^r(P) = p^{(4\cdot 4)(4+4)}(3s+2) + p^{(4\cdot 1)(4+1)}(3(sr+r)-4) + p^{(1\cdot 1)(1+1)}(3(sr-2r)+2)$$
$$RReZG_3SC_s^r(P) = p^{(16)(8)}(3s+2) + p^{(4)(5)}(3(sr+r)-4) + p^{(1)(2)}(3(sr-2r)+2) \quad (4.7)$$

After simplification of Equation (4.7), we get:

$$RReZG_3SC_s^r(P) = (16)(8)(3s+2) + (4)(5)(3(sr+r)-4) + (1)(2)(3(sr-2r)+2)$$
$$RReZG_3SC_s^r(P) = 128(3s+2) + 20(3(sr+r)-4) + 2(3(sr-2r)+2)$$
$$RReZG_3SC_s^r(P) = 384s + 256 + 60sr + 60r - 80 + 6sr - 12r + 4$$
$$RReZG_3SC_s^r(P) = 384s + 66sr + 48r + 180$$

The Reverse Atom bond connectivity polynomial and index

Using Table 2 along with Equation (2.8), we get:

$$RABCSC_s^r(P) = p^{\sqrt{\frac{(4+4-2)}{(4\cdot 4)}}}(3s+2) + p^{\sqrt{\frac{(4+1-2)}{(4\cdot 1)}}}(3(sr+r)-4) + p^{\sqrt{\frac{(1+1-2)}{(1\cdot 1)}}}(3(sr-2r)+2)$$
$$RABCSC_s^r(P) = p^{\sqrt{\frac{6}{16}}}(3s+2) + p^{\sqrt{\frac{3}{4}}}(3(sr+r)-4) + p^{\sqrt{\frac{0}{1}}}(3(sr-2r)+2) \quad (4.8)$$

After simplification of Equation (4.8), we get:

$$RABCSC_s^r(P) = \sqrt{\frac{3}{8}}(3s+2) + \sqrt{\frac{3}{4}}(3(sr+r)-4)$$

5. Reverse Degree Based TD's of Silicate Triangle Fractal Network Si_n

Table 3: Reverse degree based edge partition of silicate triangle fractal network Si_n

Types of Atom Bonds	Cardinality
E(4,4)	$3[1-3(1-3^{s-1})]$
E(4,1)	$3^{s+1}+3$
E(1,1)	3^{s+1}

The Reverse 1^{st}-Zagreb polynomial and index
Using Table 3 along with Equation (2.1), we get:

$$RM_1Si_n(P) = p^{(4+4)}(3[1-3(1-3^{s-1})]) + p^{(4+1)}(3^{s+1}+3) + p^{(1+1)}(3^{s+1})$$

$$RM_1Si_n(P) = p^{(8)}(3-9(1-3^{s-1}) + p^{(5)}(3^{s+1}+3) + p^{(2)}(3^{s+1}) \tag{5.1}$$

After simplification Equation (5.1), we get

$$\begin{aligned} RM_1Si_n(P) &= (8)(3-9(1-3^{s-1}) + (5)(3^{s+1}+3) + (2)(3^{s+1}) \\ RM_1Si_n(P) &= -8(-6+3\times 3^s) + 15(3^s) + 6(3^s) + 15 \\ RM_1Si_n(P) &= 21(3^s) + 8(3^{s+1}) - 33 \end{aligned}$$

The Reverse 2^{nd} Zagreb Polynomial and Index
Using Table 3 along with Equation (2.2), we get:

$$RM_2Si_n(P) = p^{(4\cdot 4)}(3[1-3(1-3^{s-1})]) + p^{(4\cdot 1)}(3^{s+1}+3) + p^{(1\cdot 1)}(3^{s+1})$$

$$RM_2Si_n(P) = p^{(16)}(3-9(1-3^{s-1}) + p^{(4)}(3^{s+1}+3) + p^{(1)}(3^{s+1}) \tag{5.2}$$

After simplification Equation (5.2), we get

$$\begin{aligned} RM_2Si_n(P) &= (16)(3-9(1-3^{s-1}) + (4)(3^{s+1}+3) + (1)(3^{s+1}) \\ RM_2Si_n(P) &= 16(-6+3\times 3^s) + 12(3^s) + 12 + 3^{s+1} \\ RM_2Si_n(P) &= 60(3^s) + 3^{s+1} - 84 \end{aligned}$$

The Reverse 1^{st}- hyper Zagreb polynomial and index
Using Table 3 along with Equation (2.3), we get:

$$RHM_1Si_n(P) = p^{(4+4)^2}(3[1-3(1-3^{s-1})]) + p^{(4+1)^2}(3^{s+1}+3) + p^{(1+1)^2}(3^{s+1})$$

$$RHM_1Si_n(P) = p^{(8)^2}(3-9(1-3^{s-1}) + p^{(5)^2}(3^{s+1}+3) + p^{(2)^2}(3^{s+1}) \tag{5.3}$$

After simplification of Equation (5.3), we get:

$$\begin{aligned} RHM_1Si_n(P) &= (64)(3-9(1-3^{s-1}) + (25)(3^{s+1}+3) + (4)(3^{s+1}) \\ RHM_1Si_n(P) &= 64(-6+3\times 3^s) + 25(3^{s+1}) + 25\times 3 + 4(3^{s+1}) \\ RHM_1Si_n(P) &= -309 + 4(3^{s+1}) + 267(3^s) \end{aligned}$$

The Reverse 2^{nd} hyper Zagreb Polynomial and Index
Using Table 3 along with Equation (2.4), we get

$$RHM_2Si_n(P) = p^{(4\cdot4)^2}(3[1-3(1-3^{s-1})]) + p^{(4\cdot1)^2}(3^{s+1}+3) + p^{(1\cdot1)^2}(3^{s+1})$$

$$RHM_2Si_n(P) = p^{(256)}(3-9(1-3^{s-1}) + p^{(16)}(3^{s+1}+3) + p^{(1)}(3^{s+1}) \tag{5.4}$$

After simplification Equation (5.4), we get

$$\begin{aligned} RHM_2Si_n(P) &= (256)(3-9(1-3^{s-1}) + (16)(3^{s+1}+3) + (1)(3^{s+1}) \\ RHM_2Si_n(P) &= 256(-6+3\times3^s) + 16(3^{s+1}) + 16\times3 + 1(3^{s+1}) \\ RHM_2Si_n(P) &= 816(3^s) + 3^{s+1} - 1488 \end{aligned}$$

The Reverse 1^{st} redefined Zagreb Polynomial and Index
Using Table 3 along with Equation (2.5), we get:

$$\begin{aligned} RReZG_1Si_n(P) &= p^{\frac{(4+4)}{(4\cdot4)}}(3[1-3(1-3^{s-1})]) + p^{\frac{(4+1)}{(4\cdot1)}}(3^{s+1}+3) + p^{\frac{(1+1)}{(1\cdot1)}}(3^{s+1}) \\ RReZG_1Si_n(P) &= p^{\frac{8}{16}}(3-9(1-3^{s-1}) + p^{\frac{5}{4}}(3^{s+1}+3) + p^{\frac{(2)}{1}}(3^{s+1}) \end{aligned} \tag{5.5}$$

After simplification of Equation (5.5), we get:

$$\begin{aligned} RReZG_1Si_n(P) &= \frac{8}{16}(3-9(1-3^{s-1}) + \frac{5}{4}(3^{s+1}+3) + \frac{(2)}{1}(3^{s+1}) \\ RReZG_1Si_n(P) &= \frac{8}{16}(-6+3\times3^s) + \frac{5}{4}(3^{s+1}) + \frac{5}{4}\times3 + \frac{(2)}{1}(3^{s+1}) \\ RReZG_1Si_n(P) &= \frac{31}{4}(3^s) + 2(3^{s+1}) - \frac{17}{4} \end{aligned}$$

The Reverse 2^{nd} redefined Zagreb Polynomial and Index
Using Table 3 along with Equation (2.6), we get:

$$\begin{aligned} RReZG_2Si_n(P) &= p^{\frac{(4\cdot4)}{(4+4)}}(3[1-3(1-3^{s-1})]) + p^{\frac{(4\cdot1)}{(4+1)}}(3^{s+1}+3) + p^{\frac{(1\cdot1)}{(1+1)}}(3^{s+1}) \\ RReZG_2Si_n(P) &= p^{\frac{16}{(8)}}(3-9(1-3^{s-1}) + p^{\frac{4}{(5)}}(3^{s+1}+3) + p^{\frac{1}{(2)}}(3^{s+1}) \end{aligned} \tag{5.6}$$

After simplification of Equation 5.6 we get:

$$\begin{aligned} RReZG_2Si_n(P) &= \frac{16}{8}(3-9(1-3^{s-1}) + \frac{4}{5}(3^{s+1}+3) + \frac{1}{2}(3^{s+1}) \\ RReZG_2Si_n(P) &= \frac{16}{8}(-6+3\times3^s) + \frac{4}{5}(3^{s+1}) + \frac{4}{5}\times3 + \frac{1}{2}(3^{s+1}) \\ RReZG_2Si_n(P) &= \frac{42}{5}(3^s) + \frac{1}{2}(3^{s+1}) - \frac{48}{5} \end{aligned}$$

The Reverse 3^{nd} redefined Zagreb Polynomial and Index
Using Table 3 along with Equation (2.7), we get:

$$\begin{aligned} RReZG_3Si_n(P) &= p^{(4\cdot4)(4+4)}(3[1-3(1-3^{s-1})]) + p^{(4\cdot1)(4+1)}(3^{s+1}+3) + p^{(1\cdot1)(1+1)}(3^{s+1}) \\ RReZG_3Si_n(P) &= p^{(16)(8)}(3-9(1-3^{s-1}) + p^{(4)(5)}(3^{s+1}+3) + p^{(1)(2)}(3^{s+1}) \end{aligned} \tag{5.7}$$

After simplification of Equation (5.7), we get:

$$RReZG_3Si_n(P) = (16)(8)(3 - 9(1 - 3^{s-1}) + (4)(5)(3^{s+1} + 3) + (1)(2)(3^{s+1})$$
$$RReZG_3Si_n(P) = (16)(8)(-6 + 3 \times 3^s) + (4)(5)(3^{s+1}) + (4)(5)(3) + 2(3^{s+1})$$
$$RReZG_3Si_n(P) = 444(3^s) + 2(3^{s+1}) - 708$$

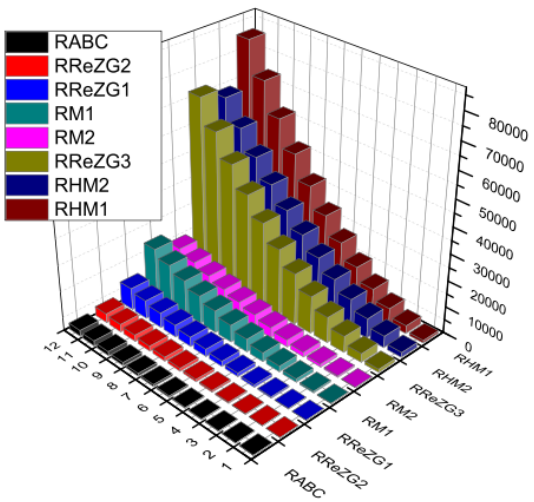

Figure 4: Graphical Comparison of Silicate Network

The Reverse Atom bond connectivity polynomial and index

Using Table 3 along with Equation (2.8), we get:

$$RABCSi_n(P) = p^{\sqrt{\frac{(4+4-2)}{(4\cdot4)}}}(3[1 - 3(1 - 3^{s-1})]) + p^{\sqrt{\frac{(4+1-2)}{(4\cdot1)}}}(3^{s+1} + 3) + p^{\sqrt{\frac{(1+1-2)}{(1\cdot1)}}}(3^{s+1})$$

$$RABCSi_n(P) = p^{\sqrt{\frac{6}{16}}}(3 - 9(1 - 3^{s-1}) + p^{\sqrt{\frac{3}{4}}}(3^{s+1} + 3) + p^{\sqrt{\frac{0}{1}}}(3^{s+1}) \tag{5.8}$$

After simplification of Equation (5.8), we get:

$$RABSi_n(P) = \frac{\sqrt{6} \times -6}{4} + 3(3^s)(\frac{\sqrt{6}}{4} + \frac{\sqrt{3}}{2})$$

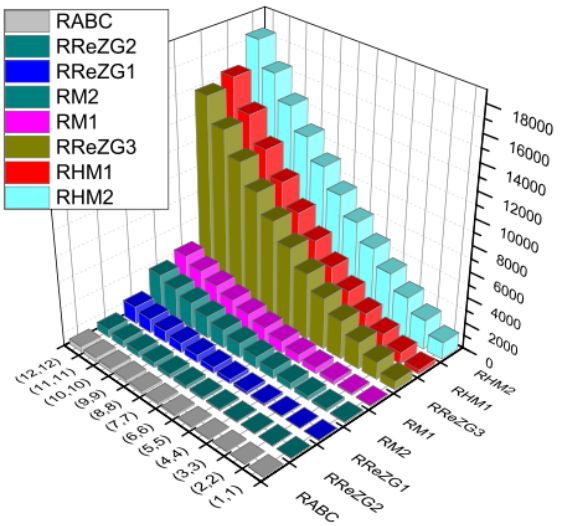

Figure 5: Graphical Comparison of Silicate Chain

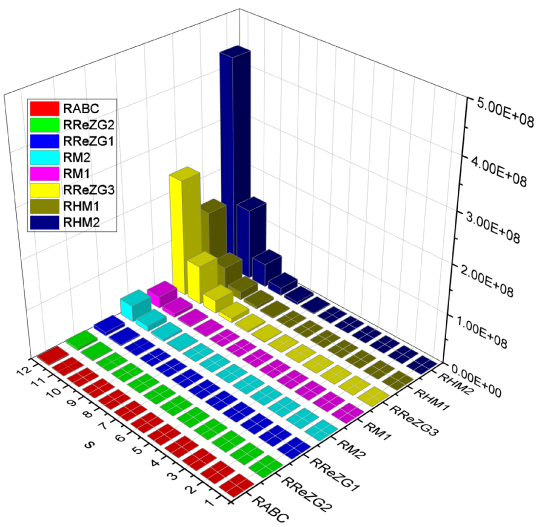

Figure 6: Graphical Comparison of Si_n

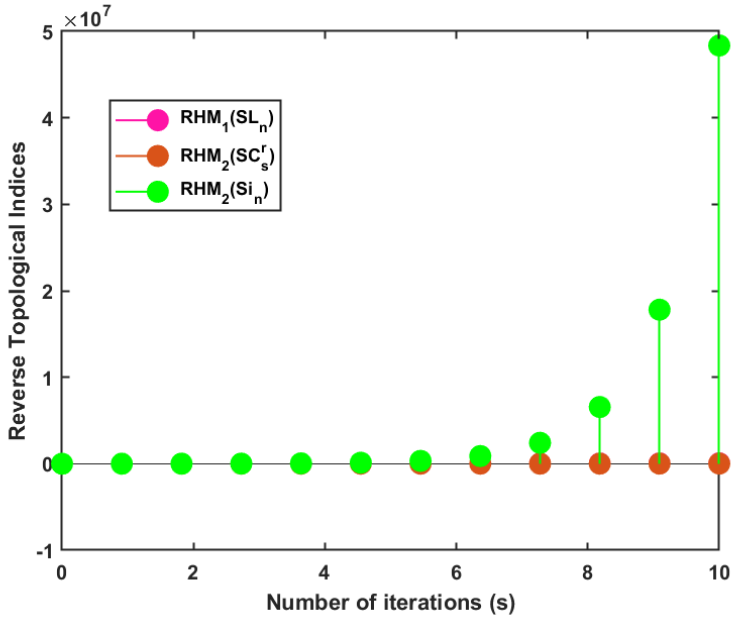

Figure 7: Graphical Comparison of SL_n, SC_s^r and Si_n

6. Numerical and Graphical Comparison of RDBTs

Tables 4 show numerical values for reverse degree-based topological descriptors (RDBTs) in SL_n.For computational reasons, we investigated s values ranging from 1 to 12. Figure 4 gives a visual depiction of the numerical results. As the value of s increased, so did the value of RDBTs.

Table 4: Numerical Computation of Topological Indices for SL_n

s	$RABC$	$RReZG_2$	$RReZG_1$	RM_1	RM_2	$RReZG_3$	RHM_2	RHM_1
1	24.4588	34.2	45	180	198	1260	1926	1008
2	80.0946	115.2	207	612	576	3312	4464	3060
3	166.9072	243	486	1296	1134	6156	7614	6156
4	284.8968	417.8	882	2232	1872	9792	11376	10296
5	434.0633	639	1395	3420	2790	14220	15750	15480
6	614.4067	907.2	2025	4860	3888	19440	20736	21708
7	825.9271	1222.2	2772	6552	5166	25452	26334	28980
8	1068.624	1584	36336	8496	6624	32256	32544	37296
9	1342.498	1992.6	4617	10692	8262	39852	39366	46656
10	1647.549	2448	5715	13140	10080	48240	68508	57060
11	1983.777	2950.2	6930	15840	12078	57420	46800	68508
12	2351.182	3499.2	8262	18792	14256	67392	63504	81000

Table 5: Numerical Computation of Topological Indices For SLC

s	$RABC$	$RReZG_2$	$RReZG_1$	RM_2	RM_1	$RReZG_3$	RHM_1	RHM_2
1	4.7939	11.1	3	87	48	678	336	1311
2	17.0233	28.2	25.5	186	138	1308	870	2274
3	34.4489	53.1	67.5	315	270	2070	1548	3339
4	57.0706	85.8	129	474	444	2964	2400	4506
5	84.8885	126.3	210	663	660	3990	3426	5775
6	117.9025	174.6	310.5	882	918	5148	4626	7146
7	156.1127	230.7	430.5	1131	1218	6438	6000	8619
8	199.519	294.6	570	1410	1560	7860	7548	10194
9	248.1215	266.6	729	1719	1944	9414	9270	11871
10	301.9202	445.8	907.5	2058	2370	11100	11166	13650
11	360.9149	533.1	1105.5	2427	2838	12918	13236	15531
12	425.1059	628.2	1323	2826	3348	14868	15480	17514

Table 6: Numerical Computation of Topological Indices For Si_n

s	$RABC$	$RReZG_2$	$RReZG_1$	RM_2	RM_1	$RReZG_3$	RHM_1	RHM_2
1	12.2	20.1	37	105	102	642	528	969
2	38.8	79.5	119.5	483	372	3342	2202	5883
3	118.7	257.7	367	1617	1182	11442	7224	20625
4	358.1	792.3	1109.5	5019	3612	35742	22290	64851
5	1076.6	2396.1	3337	15225	10902	108642	67488	197529
6	3231.9	7207.5	10019.5	45843	32772	327342	20308	595563
7	9697.7	21641.7	30067	137697	98382	983442	609864	1789665
8	29095.3	64944.3	90209.5	413259	295212	2951742	1830210	5371971
9	87288.1	194852.1	270637	1239945	885702	8856642	549124	16118889
10	261866.5	584575.5	811919.5	3720003	2657172	26571342	16474362	48359643
11	785601.6	1753745.7	2435767	11160177	7971582	79715442	4942370	145081905
12	2356806.9	5261256.3	7307309.5	33480699	23914812	239147742	148271730	435248691

Tables 5 present numerical values for reverse degree-based topological descriptors (RDBTs) in SLC. For computational considerations, we examined s values spanning from 1 to 12. Figure 5 provides a visual representation of the numerical results. RDBTs increased in value in tandem with the increase in s.

Tables 6 present numerical values for reverse degree-based topological descriptors (RDBTs) in Si_n. For computational considerations, we examined s values spanning from 1 to 12. Figure 6 provides a visual representation of the numerical results. Figure 7 shows numerical results of three structures of SL_n, SC_s^r and Si_n. RDBTs increased in value in tandem with the increase in s.

7. Conclusion

This study calculates the topological indices based on the reverse degree for the silicate network (SL_n), silicate chain SC_s^r and silicate triangle fractal network (Si_n). Using these topological invariants, we can observe a chemical molecule under investigation's physical properties, biological activity, and chemical reactivity. We plot our outcomes as well. We can get the value of the topological indices for various parameter values for the silicate network,silicate chain and silicate triangle fractal network with the use of this graphical representation of the indices. The topological descriptor of eight reverse degree-based topological indices for a molecular structure of silicate networks, silicate chain and silicate triangle fractal network is presented in this publication along with important findings. Due to the rich conceptualization, as indicated in table 4-6 and figure 4-5, we provided a numerical and graphical analysis of the topological index results acquired for a few initial values of the used parameter. Based on their values which are ascertained by mathematical calculations, numerical analysis, and graphical analysis—these descriptors are arranged in a hierarchy. Furthermore, in the numerical analysis of the correlation between the

topological index of the structure SL_n, the RHM_1 index reveals a better correlation for $s = 6$ compared to other indices. The vertex degree and maximum degree are calculated based on the SL_n graph invariance, which depicts the topological properties of SL_n. In the silicate chain SC_s^r, the correlation between the topological index and the RHM_1 index shows a strong correlation in the first iteration $s = 1$. The vertex degree and the maximum degree are determined by the invariance of the SC_s^r graph, which highlights the topological characteristics of SC_r^s.

The RHM_2 index of the silicate triangle network shows a strong correlation when comparing all indices for $s = 1$. $RABC$ provides the best approximation with fewer iterations needed to determine the number of (SiO_4) silicate structure copies and the fractal dimension of the silicate triangle fractal network. The Si_n structure ultimately offers a better correlation and illustrates the topological characteristics more effectively.

Declarations

Data Availability:

All data generated or analyzed during this study are included in this article.

Funding:

Not Applicable.

Ethics Approval:

Not Applicable.

Consent to Participate:

Not Applicable.

Consent for Publication:

The authors declare that the figures and tables used in this paper are original and are not published anywhere.

Conflict of Interest:

The authors declare that they have no conflict of interest.

Competing Interests:

The authors declare no competing interests.

Authors Contribution:

Gayathiri is involved in main result, computation and calculation. Manimaran is involved in main result and calculation verification. Abdul Rauf wrote the introduction, found resources, validation. Farhan wrote the introduction, graphs, validation and formal analysis of research.

References

1. Gutman, Ivan., *Degree-based topological indices.* Croatica chemica acta, 86(4), 351-361, (2013).
2. Furtula, B., Graovac, A., & Vukicevic, D., *Augmented zagreb index.* Journal of mathematical chemistry, 48, 370-380, (2010).
3. Gutman, I., *Total π-electron energy of benzenoid hydrocarbons.* Springer, 17(4), 29-63, (2005).
4. Balaban, Alexandru, T., Motoc, Ioan., Bonchev, Danail., Mekenyan, Ovanes., *Topological indices for structure-activity correlations.* Springer, 21-55, (2007).
5. Nikolic, S., Kovacevic, G., Milicevic, A., & Trinajstic, N., *The Zagreb indices 30 years after.* Croatica chemica acta, 76(2), 113-124, (2003).
6. Trinajstic, N., *Chemical graph theory.* CRC press, (2018).
7. Prathik., Anandhan., Uma, K., Anuradha, J., *An overview of application of graph theory.* International Journal of ChemTech Research, 9(2), 242-248, (2016).

8. Khan, A. R., Bhatti, S. A., Imran, M., Tawfiq, F. M., Cancan, M., & Hussain, S. *Computation of Differential and Integral Operators Using M-Polynomials of Gold Crystal*. Heliyon, (2024).

9. Ghani, M. U., Sultan, F., Tag El Din, E. S. M., Khan, A. R., Liu, J. B., & Cancan, M., A Paradigmatic Approach to Find the Valency-Based K-Banhatti and Redefined Zagreb Entropy for Niobium Oxide and a Metal–Organic Framework. Molecules, 27(20), 6975, (2022).

10. Khan, A. R., Awan, N. U. H., Ghani, M. U., Eldin, S. M., Karamti, H., Jawhari, A. H., & Mukhrish, Y. E. (2023). *Fundamental Aspects of Skin Cancer Drugs via Degree-Based Chemical Bonding Topological Descriptors*. Molecules, 28(9), 3684.

11. Khan, A. R., Ullah, Z., Imran, M., Malik, S. A., Alamoudi, L. M., & Cancan, M., *Molecular temperature descriptors as a novel approach for QSPR analysis of Borophene nanosheets*. PLOS ONE, 19(6), e0302157, (2024).

12. Imran, M., Khan, A. R., Husin, M. N., Tchier, F., Ghani, M. U., Hussain, S., *Computation of Entropy Measures for Metal-Organic Frameworks*. Molecules, 28(12), 4726,(2023).

13. Khan, A. R., Awan, N. U. H., Tchier, F., Alahmari, S. D., Khalel, A. F., & Hussain, S., *An estimation of physiochemical properties of bladder cancer drugs via degree-based chemical bonding topological descriptors*. Journal of Biomolecular Structure and Dynamics, 1-9, (2023).

14. Alsaadi, F. E., Salman, M., Rehman, M. U., Khan, A. R., Cao, J., Alassafi, M.O., *On the Geodesic Identification of Vertices in Convex Plane Graphs*. Mathematical Problems in Engineering, 1-13, (2020).

15. Khan A. R., Mutlib, A., Campe˜na, F. J. H., Tchier, F., Karim, M., and Hussain, S., *Investigation of reduced reverse degree based polynomials & indices of gold crystals*. Physica Scripta, 99, 075259, (2024).

16. Husin, M. N., Khan, A. R., Awan, N. U. H., Campena, F. J. H., Tchier, F., & Hussain, S., *Multicriteria decision making attributes and estimation 15 of physicochemical properties of kidney cancer drugs via topological descriptors*. Plos one, 19(5), e0302276, (2024).

17. Zhao, D., Chu, Y. M., Siddiqui, M. K., Ali, K., Nasir, M., Younas, M. T., & Cancan, M., *On reverse degree based topological indices of polycyclic metal organic network*. Polycyclic Aromatic Compounds, 42(7), 4386-4403, (2022).

18. Chu, Y. M., Khan, A. R., Ghani, M. U., Ghaffar, A., & Inc, M., *Computation of zagreb polynomials and zagreb indices for benzenoid triangular & hourglass system*. Polycyclic Aromatic Compounds, 43(5), 4386-4395, (2023).

19. Khan, A. R., Ghani, M. U., Ghaffar, A., Asif, H. M., & Inc, M., *Characterization of temperature indices of silicates*. Silicon, 15(15), 6533-6539, (2023).

20. Khan, A. R., Zia, A., Campena, F. J. H., Siddiqui, M. K., Tchier, F., & Hussain, S., *Investigations of Entropy Double & Strong Double Graph of Silicon Carbide*. Silicon, 1-11, (2024).

21. Gayathiri V,. Manimaran, A., *Computing certain topological indices of silicate triangle fractal network modeled by the Sierpiński triangle network*. Contemporary Mathematics, 5(2), 5-19, (2024).

22. Divya A,. Manimaran, A., *Topological indices for the iterations of Sierpiński rhombus and Koch snowflake*. EPJ ST, 230(12), 3971-3980, (2021).

23. Kulli, V. R., *Computation of some topological indices of certain networks*. International Journal of Mathematical Archive, 8(2), 99-106, (2017).

24. Jung, C. Y., Gondal, M. A., Ahmad, N., & Kang, S. M., *Reverse degree based indices of some nanotubes*. Journal of Discrete Mathematical Sciences and Cryptography, 22(7), 1289-1294, (2019).

25. Wei, J., Cancan, M., Rehman, A. U., Siddiqui, M. K., Nasir, M., Younas, M. T., & Hanif, M. F., *On topological indices of remdesivir compound used in treatment of Corona virus (COVID 19)*. Polycyclic Aromatic Compounds, 42(7), 4300-4316, (2022).

26. Hakeem, Abdul., Katbar, Nek Muhammad., Shaikh, Hisamuddin., Tolasa, Fikadu Tesgera., Abro, Oshaque Ali., *Reverse degree-based topological indices study of molecular structure in triangular Υ-graphyne and triangular Υ-graphyne chain*. Frontiers in Physics, 12, 1422098, (2024).

27. Kavitha Kolekar Chandrashekar, Jagatheswari Srirangan, *Topological Properties and Computation of Silicate Networks Using Graph-Invariants*. MATCH Commun. Math. Comput. Chem., 93, 463-497, (2025).

Gayathiri Vasudevan,
Department of Mathematics,
School of Advanced Sciences,
Vellore Institute of Technology,
Vellore - 632 014,
Tamil Nadu, India.
E-mail address: raj.gaya04@gmail.com

and

Manimaran Angamuthu (Corresponding author),
Department of Mathematics,
School of Advanced Sciences,
Vellore Institute of Technology,
Vellore - 632 014,
Tamil Nadu, India.
E-mail address: marans2011@gmail.com

and

Abdul Rauf Khan,
Department of Mathematics,
Faculty of Sciences,
Ghazi University,
Dera Ghazi Khan - 32200, Pakistan.
E-mail address: khankts@gmail.com

and

Farhan Qadir,
Department of Mathematics,
Faculty of Sciences,
Ghazi University,
Dera Ghazi Khan - 32200, Pakistan.
E-mail address: farhanqadir521@gmail.com